

Multi-Entity Registration of Point Clouds for Dynamic Objects on Complex Floating Platform using Object Silhouettes

Feng Wang, Han Hu, Xuming Ge, Bo Xu, Ruofei Zhong, Yulin Ding, Xiao Xie, Qing Zhu

Abstract—This paper is focused on a challenging topic emerging from the registration of point clouds, specifically the registration of dynamic objects with low overlapping ratio. This problem is especially difficult when the static scanner is installed on a floating platform, and the objects it scans are also floating. These issues make most of the automatic registration methods and software solutions invalid. To solve this problem, explicit exploration of the static region is necessary for both the coarse and fine registration steps. Fortunately, determining the corresponding regions can be eased by the intuitive realization that in urban environments, natural objects neither present straight boundaries nor stack vertically. This intuition has guided the authors to develop a robust approach for the detection of static regions using planar structures. Then, silhouettes of the objects are extracted from the planar structures, which assist in the determination of an SE(2) transformation in the horizontal direction by a novel line matching method. The silhouettes also enable identification of the correspondences of planes in the step of fine registration using a variant of the iterative closest point method. Experimental evaluations using point clouds of cargo ships with different sizes and shapes reveal the robustness and efficiency of the proposed method, which gives 100% success and reasonable accuracy in rapid time, suitable for an on-line system. In addition, the proposed method is evaluated systematically with regard to several practical situations caused by the floating platform, and it demonstrates good robustness to limited scanning time and noise.

Index Terms—Terrestrial laser scanning; Point clouds registration; Change detection; Plane detection; Line matching

I. INTRODUCTION

POINT clouds obtained by terrestrial laser scanners (TLS) have emerged as one of the most widely used datasets for various three-dimensional (3D) applications, such as 3D

Manuscript received: June 28, 2020. This work was supported by the National Natural Science Foundation of China (Projects No.: 41631174, 61602392, 41371434), the National Key Research and Development Program of China (Project No.: 2018YFB0505404) and the Provincial Key Research and Development Program of Sichuan (Project No.: 2018SZ0339). (*Mutual corresponding authors: Han Hu and Xuming Ge*).

F. Wang, H. Hu, X. Ge, B. Xu, and Y. Ding are with the Faculty of Geosciences and Environmental Engineering, Southwest Jiaotong University, Chengdu, China (e-mail: wangfeng19920903@my.swjtu.edu.cn; han.hu@swjtu.edu.cn; xuming.ge@swjtu.edu.cn; xubo@swjtu.edu.cn; rainforests@126.com).

Ruofei Zhong is with the Beijing Advanced Innovation Center for Imaging Technology, Capital Normal University, Beijing, China (e-mail: zrfss@163.com).

Xiao Xie is with Zhejiang Hi-target Space Information Technology Co. Ltd., Huzhou, China (e-mail: xiexiao@zjzh.com).

Qing Zhu is with the Faculty of Geosciences and Environmental Engineering, Southwest Jiaotong University, Chengdu, China and also with the Beijing Advanced Innovation Center for Imaging Technology, Capital Normal University, Beijing, China (e-mail: zhuc66@263.net).



Fig. 1: The TLS is installed on the pumping ship to monitor the changes of the cargo ship (a), slanted with a pitch angle δ to increase the field of view (b).

model reconstruction [1], [2], forest biomass estimation [3], [4], extraction of street-level static scene semantics [5], [6] and change monitoring [7], [8]. The registration of point clouds [9], which involves fusing multiple scans from different locations or times to the same coordinate frame, is a prerequisite for the above applications. This paper is focused on the registration of dynamic objects on a floating platform for the estimation of volume changes of cargo ships, e.g., the volume of river sands pumped from another ship (Fig. 1). First, the empty cargo ships are pre-scanned and stored in the database; next, during on-line operation, the corresponding point clouds and all of the auxiliary information are recognized using radio-frequency identification (RFID) and reloaded as querying dataset; then, after loading, the cargo ship is re-scanned using the TLS installed obliquely on the sand-pumping ship (Fig. 1b) and detected from the background; finally, the two point clouds are compared and the change in volume is computed.

A. Objectives

During the past two decades, several algorithms have been developed for point cloud registration [10]–[12], such that the coarse-to-fine registration strategy is now sufficiently mature to solve problems in common scenarios. The strategy involves a global registration step to obtain a reasonable initial estimation, e.g., by geometry- [13]–[15] or descriptor-based [16], [17] methods, and a local step to refine the misalignment, e.g., using a method from the iterative closest point (ICP) family [18]–[20]. Despite the plethora of solutions [21], [22] used in the industry, however, we have not yet seen a feasible and reliable method to automatically solve the registration of dynamic objects. Although recent studies, e.g., Qin and Gruen [7] and Ge [8], have pioneered approaches for registration of point clouds of dynamic objects, several key problems still remain, as follows:

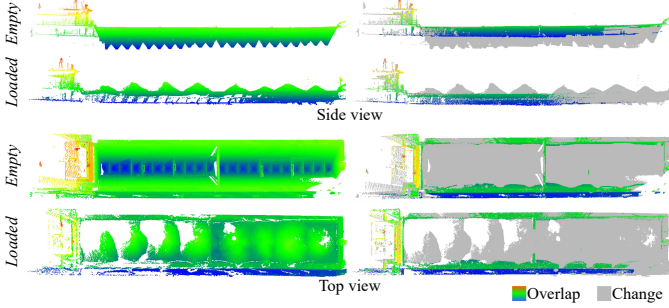


Fig. 2: The problem of low overlap ratio caused by dynamic scenes, e.g., less than 25% in the above case. The colored and gray points indicate overlapped and changed regions, respectively.

a) Low overlapping ratio: In the registration of static scenes, viewpoint differences result in variation of the overlapping regions, which can be controlled by appropriate configurations of the locations of multiple scans. However, this is unfeasible for dynamic objects (Fig. 2). Because changed regions need to be excluded from the registration, mutual structure analyses dependent on domain specific knowledge are required.

b) Inhomogeneity of point clouds: In the case of a TLS on a ground platform, the density of point clouds is inhomogeneous because of non-uniform distances between the objects and scanner. Additionally, the point clouds are collected on an unstable platform, and the data must be assumed to contain noise. Because the density of the point clouds near the scanner is, in general, unnecessarily high, the inhomogeneity may be alleviated by controlling the scanning speed and resampling to a consistent resolution. However, extending the scanning time is not a viable remedy for a TLS mounted on a floating platform, as the asynchronous motion of the two ships will often lead to breakage effects, as shown in Fig. 3. Therefore, the registration methods should be robust to the inhomogeneity of density both inside the same point cloud and between different scans; however, commonly used point features are inherently sensitive to data noise and inhomogeneity.

c) Runtime requirement: Most point-based registration methods adopt a certain variant of the random sample consensus (RANSAC) strategy [23], for which early-termination criteria are not well defined. In general, the algorithms have to reach a prescribed number of iterations or running time before stopping. Because of the large number of points (or keypoints), a single pair of registrations may require up to several minutes, and the standard deviations of the running time for different cases are also generally large, which is not suitable for an on-line system. Therefore, a more reliable and stable registration pipeline should be considered.

B. Related Works

For brevity, in this paper we introduce only the most closely related works on pairwise registration and refer the interest readers to the extensive reviews on other topics [9], [12].

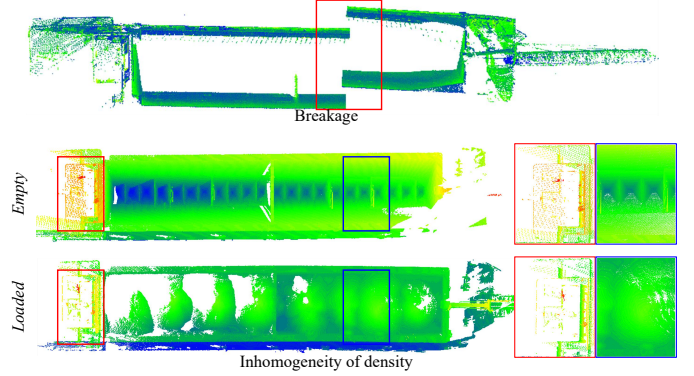


Fig. 3: The problem of inhomogeneity of point clouds caused by the floating platform. The scanning time cannot be extended because of the breakage effect, and the inhomogeneity of point cloud density exists both inside the same point clouds and between the empty and loaded scans.

a) Coarse registration: To find the initial transformation between two point clouds, two categories of approaches are generally used: geometry- and descriptor-based methods. The simplest approach [24] among the former is to exhaust all of the configurations of three keypoints in a RANSAC [25] paradigm. To alleviate the prohibitively long time requirements, the strategy of the 4-points congruent set (4PCS) was proposed [23] and subsequently extended [8], [13], [14]. With respect to the latter category, the descriptors are generally computed using the statistics of the normal vectors, distribution and density of the point clouds [6], [10], [26]. Therefore, planar structures are problematic, because their distinctiveness is extremely low; in general, large planar regions are simply removed by the descriptor-based methods [27]. In addition, 3D keypoint detectors [28], [29] are considered to have poorer repeatability than their 2D counterparts [9], [30]. However, both of the above categories of point-based methods – those using geometric inference [31] or descriptor searching [16] – have unstable performances in both accuracy and running time, and fail often in certain scenarios.

b) Fine registration: After obtaining the initial transformation, local methods are used to refine the results, which are in general less challenging than the coarse registration. The ICP methods family [18] is the most widely adopted for this purpose, which can also support planes [32], [33], normal vectors [34], [35], global information [20] and colors [36]. ICP is inherently sensitive to the overlap ratio, especially for changed objects [9], [32]; however, specific strategies may be adopted to increase the robustness of ICP [37].

c) Registration based on structures: In urban environments, where objects are intricately structured, the performance of keypoint detectors and descriptors may decrease significantly [9], [31]. The findings of recent studies confirmed that semantic features, which reveal the structures of architectural objects, were superior to natural keypoints [12], [15], [31] for urban applications. However, the semantic points are generally designed for buildings, which present clear corners or useful information in horizontal profiles [38]; in addition, the existing approaches are still based on low-

level point features and are sensitive to the severe noise and inhomogeneity of the point clouds. Aside from points, high-level structures have also been adopted that are less sensitive to the influence of point cloud quality. For instance, Yang et al. [39] proposed a registration method using the outlines of buildings, which could even handle the challenging cases of aerial-ground integration. Yang et al. [39] have inspired our work in the direction of further exploring the approaches to matching line segments for 2D images [40]–[43], even when no color information is available surrounding the line segments extracted from the TLS point clouds.

C. Contributions

To solve the above issues, we propose a novel multi-entity registration method for the point clouds of dynamic objects collected on a floating platform using silhouette information. To manage the low overlapping ratio, by exploiting the fact that artificial structures generally comprise planar structures with straight lines, while natural objects are irregular, we propose a robust method to segment the planar parts and extract the straight silhouettes. The subsequent steps of global and fine registration are both based on the line and plane entities. Because line and plane entities are higher-level abstractions of the objects than their point features, these entities are intrinsically less sensitive to the defects of the point clouds. For the coarse registration, we first use the geometric relationships of the 2D silhouettes to horizontally align the point clouds; then, the vertical offsets are compensated using horizontal planes. For the global registration, we first estimate the matching of 3D planes that are detected mutually in both point clouds, followed by an improved point-to-plane ICP [19]. The volume changes are then estimated in a pre-defined region of the queried cargo ships stored in the database.

In summary, the main contributions of our method comprise: 1) a hierarchical strategy to carry out the registration, i.e., first detecting and then matching, which reduces the searching space and increases the reliability of the registration; 2) the adoption of 2D object silhouettes of the ships to overcome the noise from the floating environment and then use of the inherent structural information of the ship to register two point clouds robustly when the overlapping ratio is low; and 3) a robust similarity-measuring metric and match-searching method of the object silhouettes to coarsely register the ships, based on line-junctions [42]. In the following, the workflow and then the three steps involved are elaborated in Section II, and in Section III, we report the experimental evaluations and analyses. Concluding remarks are presented in Section IV.

II. MULTI-ENTITY REGISTRATION OF POINT CLOUDS FOR DYNAMIC OBJECTS

This paper aims to provide an automatic, efficient and reliable method for the on-line registration of point clouds between loaded and pre-scanned empty cargo ships. A TLS is installed obliquely on river sand pumping ship adjacent to cargo ships as shown in Fig. 1. In addition, due to the limited operation time and safety issues, no artificial target is allowed. All of the pre-scanned models of the cargo ships are

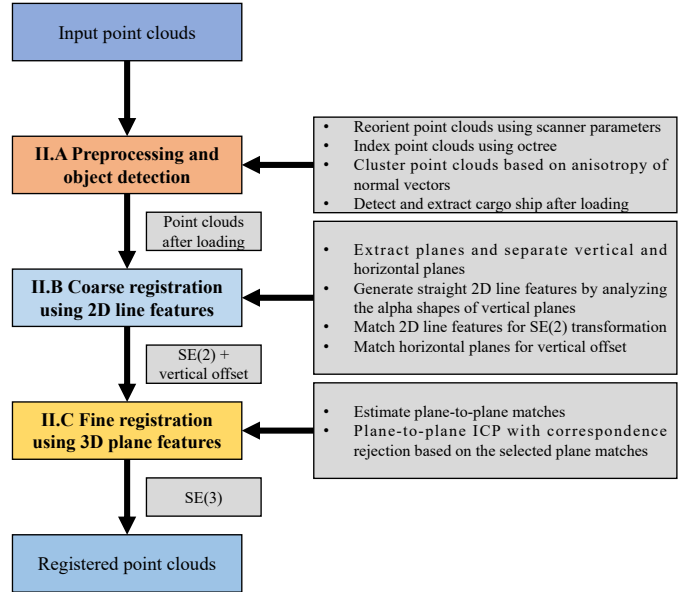


Fig. 4: Workflow of the proposed multi-entity point clouds registration method.

stored in the database and the corresponding model is detected using RFID and streamed into the main memory from the database. After registration, the changed volume between the model and loaded cargo ships is estimated in a 2.5D fashion by the gridded digital surface model (DSM). Because the step for volume estimation is relatively trivial, this paper is focused on the method for the registration of point clouds, which consists of three major steps as shown in Fig. 4: detection of the cargo ship, coarse registration and fine registration.

A. Preprocessing and object detection

Because the TLS is installed obliquely, the point clouds are first leveled using the angle δ as shown in Fig. 1. Specifically, the rotation matrix $R = \begin{pmatrix} \cos \delta & 0 & -\sin \delta \\ 0 & 1 & 0 \\ \sin \delta & 0 & \cos \delta \end{pmatrix}$ is applied to the point clouds. In addition, similar to most registration methods of point clouds [11], [12], we use an octree to resample the point clouds to a specified resolution, which is determined empirically and fixed at 10 cm.

As shown in the top left of Fig. 5, it is quite common for several cargo ships to be queued adjacently, and the first step is the separation of the target ship from the background. For point clouds of cargo ships, the normal vectors of the ships themselves (which are calculated by local points) are relatively regular, while the objects connecting the ships are tortuous and small, and their normal vectors appear irregular and anisotropic, as shown in the middle row and enlarged views of Fig. 5. Herein, we propose an efficient method to filter out the small objects between ships based on sample anisotropy, where anisotropy is defined by the differences between normal vectors in a local neighborhood. Specifically, the curvature and normal vector for each point are first obtained through the standard eigen-decomposition and the points are sorted ascendingly by their curvatures. Then, beginning with the point with the smallest curvature, we test the average direction of

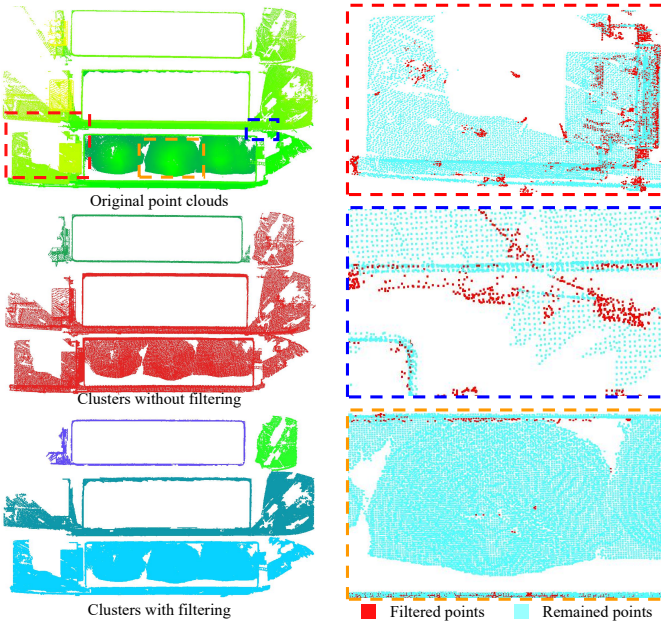


Fig. 5: Clustering and detection of the target objects. The left column shows the clustering results with and without the proposed filtering process. The right column shows the three enlarged views of different parts of the ships.

the normal vectors of the K-nearest neighbors (KNN, $K = 30$) against the current point: if the angle difference is larger than a threshold (15° is used), this point is pushed into the filtered points set; otherwise it is preserved. The right column of Fig. 5 shows the filtered and preserved points sets in red and cyan, respectively.

After filtering the small objects, we use the Euclidean clustering methods implemented in the PCL library [44] to separate different objects, and the nearest cluster to the scanner is chosen as the target. Note that because a rigorous threshold is used in the filtering, some useful points may also be excluded, as shown in the bottom right of Fig. 5. The filtered points are then assigned to the nearest cluster before subsequent point clouds registration.

B. Coarse registration using silhouettes

After extracting the target object and reloading the recognized model from the database using RFID, the next step is to register the two models. We have developed a two-step method for the coarse registration based on 2D line segments that represent the approximate silhouettes of the objects. Fig. 6 demonstrates the workflow of the coarse registration, which estimates an SE(2) transformation and vertical offset using the extracted entities. The two steps as illustrated in Fig. 6 (b) through (d) are described in the following subsections.

1) Extraction and refinement of the planar structures and silhouettes: The fundamental step for the registration of changed point clouds is the selection of regions that are static during the two phases of data collection; in this context, it is generally assumed that man-made objects consist of planar structures. Therefore, this research is focused on planes and the derivatives of planes, e.g., the 2D straight lines that represent

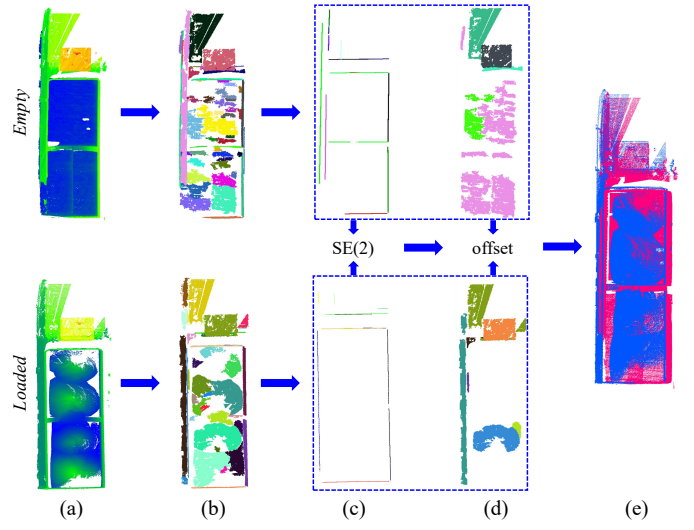


Fig. 6: Workflow of the coarse registration. From (a) the original point clouds, we first extract (b) planar patches. Then, the planar patches are used to extract (c) the silhouettes of the objects as described in Section II-B1. Assuming that the point clouds are approximately leveled, the 2D silhouettes are used to estimate an SE(2) transformation that aligns the two objects horizontally, followed by a vertical offset using (d) the planar patches (Section II-B2). Finally, using both the SE(2) transformation and vertical offset, (e) the point clouds are aligned initially.

the silhouettes of the objects, in the procedure of point clouds registration. Another merit of using plane and line entities rather than points is that high-level entities are more robust to data inhomogeneity and noise.

Specifically, both the improved region growing methods [45] and RANSAC-based methods [46] suffice for this objective; empirically, region growing-based methods have more stable performances and recall rates than RANSAC approaches at the cost of slightly longer runtime. In addition, as noted in Fig. 6b, planes are not solely sufficient to separate the static and dynamic areas, as the loaded areas will also include some spurious planes. To fix this issue, additional knowledge is used to distinguish the static and dynamic areas: (1) objects with straight boundaries are more likely to be man-made and (2) natural objects seldom stack near-vertically.

For point (1) in the previous paragraph, non-horizontal and non-vertical planes are filtered by an empirical threshold (10°) and the remainder are refitted to the axis-aligned directions in the process of coarse registration. The alpha shapes [47] of the horizontal planes are extracted, which are represented by polylines; the polylines are simplified and regularized using the hierarchical optimization approach [48] and the threshold is determined by the resolution of the voxel grids. The straightness of the simplified polylines is characterized by the length of the segments and only those with edges exceeding 2 m are considered in the subsequent processes. For point (2) in the previous paragraph, taking advantage of the scarcity of vertical objects in natural scenes, the axis-aligned vertical planes are directly projected to the horizontal planes.

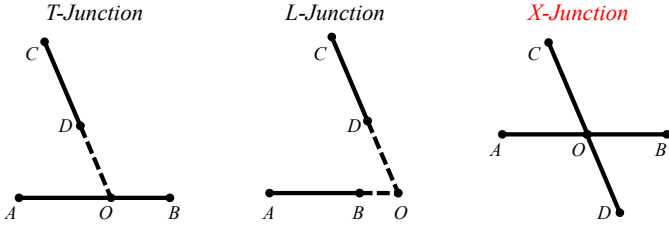


Fig. 7: Three types of line-junctions for the coarse registration. The *X-Junction* is not considered in this paper and a *T-Junction* is divided into two *L-Junctions* in the process of coarse registration. The solid parts indicate the extracted segments and the dashed parts are the extension of lines.

The silhouettes representation comprises only the projected lines of the vertical planes, while the horizontal planes are used to estimate the vertical offset.

2) *Coarse registration using 2D silhouettes*: Although a large amount of research has been performed to examine the problem of image matching using line features, most methods require photometric information to compute the descriptors [42] or to measure the similarities [40], [43]. However, photometric information is not available for extracted silhouettes. The few methods that solely exploit geometric information may be too restrictive in the case of point clouds, e.g., either requiring multiple views to cluster the line segments [41] or the preservation of the lengths of the segments obtained from different views [49], [50]. In the following, we demonstrate our novel method for the coarse registration of 2D silhouettes without the above restrictions, which comprises (1) formulation of the entities for matching, (2) measuring the similarities of the entities, (3) matching the entities using the RANSAC paradigm and (4) estimation of the vertical offset.

a) *Line junctions for the coarse registration*: Because of the difficulty of establishing the correspondences of a single line, we were inspired by previous works [42], [49] to adopt the concept of line-junctions. A line-junction is a pair of intersecting lines, for which the position of the intersection lies within a certain buffer of the segment [42]. In addition, the method presented herein requires that the intersections reside inside the minimum-area rectangle of the point clouds, as otherwise the point is not capable of being a physically valid intersection. Although, as shown in Fig. 7, three types of junctions can exist between two lines, we have found that for the intersections of silhouettes extracted from point clouds, the *X-Junction* is rather rare because structures seldom cross each other in 3D space. Therefore, only the *T-Junction* and *L-Junction* are considered, and in addition, a *T-Junction* is divided into two *L-Junctions*, i.e., $\angle AOC$ and $\angle BOC$. In the procedure of coarse registration, we only have to consider the *L-Junction* entities, i.e., a set of *L-Junctions* $\mathcal{L} = \{L_i\}$ is generated from the silhouettes.

b) *Similarity of a pair of *L-Junctions**: After defining the entities used for coarse registration, the next step is measuring the similarity of a pair of *L-Junctions* (L, L'), which is essential for line matching. For this purpose, most researchers have used photometric measurement of images [42], [43], which generally falls into two categories of methods: the SIFT-like

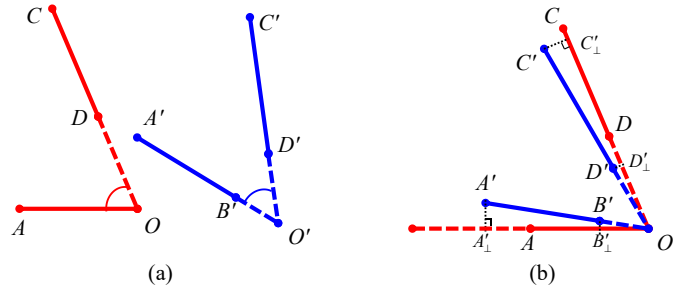


Fig. 8: Illustration of the method for estimating the similarities between (a) two *L-Junctions*, where the two *L-Junctions* are first aligned in a least-squares manner and the similarities are estimated based on the (b) intersected segments and difference of angles. To illustrate properties of different types of junctions, the red junction is chosen to be segmented from a *T-Junction*.

descriptors and the correlations of image intensities. However, the above methods are not suitable for our purposes. Instead, in this research, we use only the lengths of the segments and the angles of the *L-Junctions*. As shown in Fig. 8a, first, false matches are pruned using the difference of the angle $\Delta\theta = |\theta - \theta'|$; only pairs with $\Delta\theta < 15^\circ$ are considered for further processing. Second, we register the two *L-Junctions* in a least-squares manner: (1) the line correspondences are chosen arbitrarily, e.g., we assume \overline{OA} matches with $\overline{O'A'}$ or $\overline{O'C'}$, as long as the lengths are similar (15%); (2) the shift o and the rotation angle τ are estimated by minimizing the projected distances between the line correspondences with O and O' aligned. For brevity, we assume \overline{OA} matches $\overline{O'A'}$ and the objective function is,

$$\min_{o, \tau} \|\overline{A'A'_\perp} + \overline{B'B'_\perp} + \overline{C'C'_\perp} + \overline{D'D'_\perp}\|^2, \quad (1)$$

where the subscript \perp indicates the pedal point. The corner induced by *T-junction* is ignored. Third, we compute the similarity based on the intersection over union (IoU) between the projected line segments, which is also weighted by the angle difference $\Delta\theta$; for the case of Fig. 8b, the similarity s is,

$$s(L, L') = \cos \Delta\theta \frac{\overline{AB'_\perp} + \overline{C'_\perp D}}{\overline{A'_\perp O} + \overline{CD'_\perp}}. \quad (2)$$

Note that, in general, a pair of *L-Junctions* may have two possible similarities (s_1, s_2). Specifically, these are $s_1 \geq s_2$ based on different choices of line correspondences, and we prune s_2 if $s_2 < 0.8s_1$, otherwise both are preserved; this strategy is inspired by the ratio matching for SIFT descriptors [30]. In addition, the byproducts of the similarity computation are the initial SE(2) transformations (o, τ), which are also recorded and used for the subsequent RANSAC-based coarse registration.

c) *RANSAC matching of *L-Junctions**: The RANSAC-based matching is inspired by the implementation of the PCL library [44] and fast global registration [16]. For the matching of point clouds, we generally choose multiple candidates for a feature rather than only a single candidate, to increase the recall rate of matches, and rank these candidates by their

similarities in the registration procedure [44]. In this paper, a maximum of two most similar *L-Junctions* are searched for the reference datasets (denoted as the matches set \mathcal{M}). Although, as indicated above, a single *L-Junction* can already determine the SE(2) transformation, we have found that using two candidates enables convergence to be achieved much faster, because two candidates allow us to prune a large amount of false configurations before testing the score of the match quality. Similar to the work by Zhou *et al.* [16], the first step requires all of the configurations with two *L-Junction* matches to be enumerated, which form the full correspondence set \mathcal{C}_F . Then we test the *compatibility* of the two matches in a configuration: if the SE(2) transformations of the two matches deviate too much from each other, this configuration is pruned; specifically, we remove the configurations for which the difference of the offset Δo (or the difference of angle $\Delta \tau$) exceeds 5% of the extent of the bounds (or 5° , respectively). The *compatible* correspondence set is indicated as \mathcal{C}_C and the average SE(2) transformation for the two matches is used for the subsequent coarse registration.

Although a least-squares solver with robust estimation could be used to solve the final SE(2) transformation using the *compatible* set \mathcal{C}_C , as evidenced by [16], we find that the RANSAC approach is more robust. The RANSAC approach we use is quite similar to the classical image-matching method based on feature points [51]: (1) A random configuration is chosen from the *compatible* set \mathcal{C}_C and all of the line segments from the matching set \mathcal{M} are warped using the corresponding SE(2) parameters; (2) The number of good matches in the matches set \mathcal{M} is directly taken as the score, where “good” is defined by the thresholds for the differences of offset and angle (1 m and 5° are used, respectively); (3) Steps (1) and (2) are iterated until a specified running time is reached or all of the configurations in \mathcal{C}_C are exhausted, and the match with the largest score is chosen. Because the number of line segments is much smaller than that for point-based methods [31], the runtime of the RANSAC procedure is relatively fast. As it is not possible to guarantee the success of coarse registration, the results are confirmed interactively by the user in the on-line pipeline; otherwise, we allow the operator to select a pair of *L-Junctions* for coarse registration.

d) Estimation of the vertical offset: Although the point clouds are leveled, the vertical offset should also be estimated, because the TLS scans at different heights before and after loading. For the estimation of the vertical offset, the horizontal planes are used. Specifically, all of the planes with an IoU larger than 30% are considered as correspondence. The reason for using such a low IoU threshold is partial occlusion. The vertical offset is then computed from the weighted average of all of the corresponding planes, for which the weights are determined according to both the IoU and the areas of the planes.

C. Fine registration using 3D plane features

The overlapping ratio of the point clouds is a crucial factor for a successful fine registration. The minimum amount of overlapping areas should generally be greater than 50% for

the classical ICP registration [37], otherwise ICP may be trapped by local minimum or non-convergence. In our cases, overlapping ratios are generally below 40% (Fig. 1), the static parts must be identified before the ICP registration. Fortunately, in the above coarse registration, we have already established correspondences for both horizontal and vertical planes.

The original point clouds are used for the fine registration, rather than the refitted and axis-aligned point clouds in coarse registration; coarse registration provides the initial position for fine registration. Although the mutual planar structures are selected as the input to the subsequent fine registration, there are still inconsistent areas that may significantly affect the efficiency and accuracy. Trimmed ICP [37] is efficient when facing this kind of inconsistency, but the accuracy of the registered results is susceptible to noise. Conversely, the point-to-plane ICP [19] is robust to noise but susceptible to inconsistency. Therefore, we combine two approaches to reject outliers that are commonly used in the ICP procedure: (1) trimming and (2) normal rejection, both of which are implemented with PCL [44]. Conventional ICP assumes that all of the points can be paired, which is unfortunately not tenable for dynamic objects with significant differences in density. Therefore, a certain number of correspondences should be removed during ICP, based on the overlapping ratio of the selected planes. The points for removal are selected by ranking the residuals and the removed percentage is computed by the estimated overlapping ratio. In addition, the normal vectors are also considered: if the difference of normal vectors between a point and a plane exceeds 10° , this point is not considered.

III. EXPERIMENTAL EVALUATIONS

To verify the effectiveness of the proposed method, we collect point clouds of four cargo ships with various shapes and sizes. Because no targets or markers are used, reference is made by off-line manual registrations in industry-approved software [21] and compared with the proposed method for qualitative and quantitative evaluations; a variant of the 4PCS using semantic keypoints (denoted as sk-4pcs below) [31] is also compared. In addition, we study and analyze the performances of the proposed method systematically with regard to various practical issues caused by the floating platform, such as the scanning time and passive movements of the objects. All of the timings recorded are conducted on a computer with 32 GB memory and a CPU with 4 cores @2.60 GHz.

A. Experimental results

The datasets of the four cargo ships are captured using the HS450 laser scanner system [52] with a field of view of 360° and 100° for the horizontal and vertical directions, respectively; the maximum scanning range is 450 m and the maximum range accuracy is 5 mm. To decrease effects due to the floating environment, the scanner is tuned in a fast scanning mode with scanning time strictly controlled below 30 s; in the above settings, the average spacing between adjacent points is approximately 2 cm. More detailed descriptions of the datasets are illustrated in Table I and the point clouds are shown in Fig. 9.

TABLE I: Details of the four pairs of point clouds for the cargo ships.

#Ship	Density(<i>points/m</i> ²) Empty	Density(<i>points/m</i> ²) Loaded	Length × Width (m)	Changed ratio (%)
1	873	720	90 × 12	78.8
2	1985	1681	54 × 10	67.2
3	1229	1164	72 × 10	69.3
4	1755	1327	54 × 10	68.4

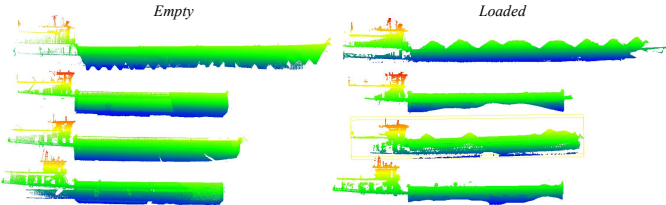


Fig. 9: The point clouds of the empty and loaded cargo ships, which are colored by height.

1) *Qualitative evaluations*: For the qualitative analyses, we demonstrate the registered point clouds for all four ships in Fig. 10, where the red and blue labels indicate point clouds before and after loading, respectively. Two vertical profiles are also plotted for both the cabin and cargo areas; note that for both regions, the point clouds are registered relatively well, even for the changed cargo areas. The only exception is the second profile of the third ship, which was caused by slight movement of the ship during the data collection.

We also compare the results from the proposed on-line pipeline and off-line manual registration in Autodesk Recap [21]. Even for an industry-approved solution with interactively selected points for coarse registration, it is still difficult for Recap to handle the fine registration using ICP; therefore, we use the automatically selected static parts for the registration and use the obtained SE(3) transformation directly. The comparisons between the two methods are shown in Fig. 11; similar to Fig. 10 we also plot the profiles inside the rectangles. From the profiles, we find that the edges of the cargo area are registered satisfactorily and that the cabin regions also present relatively consistent results.

2) *Quantitative evaluations*: We first quantitatively evaluate the registration accuracy with regard to the reference. We record both point-wise translational residuals in the trimmed point-to-plane ICP and the rotation error of the SE(3) transformation between the proposed method and reference, where the calculation of the rotation error is taken from previous works [10], [12] as Equation

$$\epsilon_R = \arccos \frac{tr(\epsilon_R) - 1}{2}, \quad (3)$$

where ϵ_R is the rotation part of the SE(3) transformation. The minimum translational error is limited by the accuracy of the sensor, and the maximum for all the four ships is approximately 1 voxel size (e.g. 10 cm), which means we have reached satisfactory results for the challenging datasets. The RMSE values of translational error and rotational error range from 20 mm to 56 mm and 20 mdeg to 70 mdeg, respectively. The worst performance is again obtained for the

TABLE II: Translation and rotation errors between the proposed on-line and off-line interactive results.

#Ship	Translation Error (mm)			Rotation Error (mdeg)	
	Minimum	Maximum	Average	RMSE	
1	8.2	29.1	20.2	20.4	19.8
2	4.2	56.5	20.6	22.8	47.6
3	2.2	119.1	51.8	56.4	70.6
4	8.4	57.6	23.3	24.9	18.9

third ship, as indicated in the qualitative evaluations. The registration accuracy is also intuitively represented by the volume differences between the proposed method and the reference. As shown in Table III, the differences almost never exceed 1% of the total volume; this conforms to the expected accuracy.

Another important issue is the robustness of the algorithm. In fact, we have experimented extensively with many publicly available algorithms, such as 4pcs [23], k-4pcs [14] and FPFH [26], which are available in PCL, [44] and Open3D [53]; however, all of the above methods failed in the coarse registration. This is expected, because none of these methods consider the structural information, but instead use natural keypoints. In the experiments, we found that the only exception was the sk-4pcs method [31], which extracts semantic keypoints that abstract the structures with points. Because sk-4pcs also uses the RANSAC approach and feeds different seeds to increase the generalization ability, its convergence performance tends to fluctuate, and thus an average of 10 runs was recorded. Table IV compares sk-4pcs and the proposed method with regard to both the successful registration rate (SRR) and runtime performances. It can be seen that the proposed method achieves relatively stable performances during the RANSAC procedure, but sk-4pcs fails occasionally. With regard to the runtime performance, even though sk-4pcs succeeds in all runs, the proposed method is still comparable with sk-4pcs, and exceeds it by a large margin whenever sk-4pcs has non-convergent searches. Note that the coarse registration procedure of the proposed method also includes extraction of the silhouettes; the registration procedure is only a small fraction of the runtime, i.e., less than 2 s in most cases.

TABLE III: Measurements of the sands volume of the cargo ships.

#Ship	Volume (<i>m</i> ³)	Difference (%)
1	1234.7	0.19
2	553.1	0.70
3	614.9	2.55
4	814.2	0.04

B. Analyses on floating platform

The above experimental results on cargo ships reveal the capability and reliability of our approach. To assess the performances of the proposed approach in a floating environment, e.g., where passive movements are caused by the waves of a river, we turn to synthetic data sets and carry out quantitative comparisons under controlled conditions. To that end, we

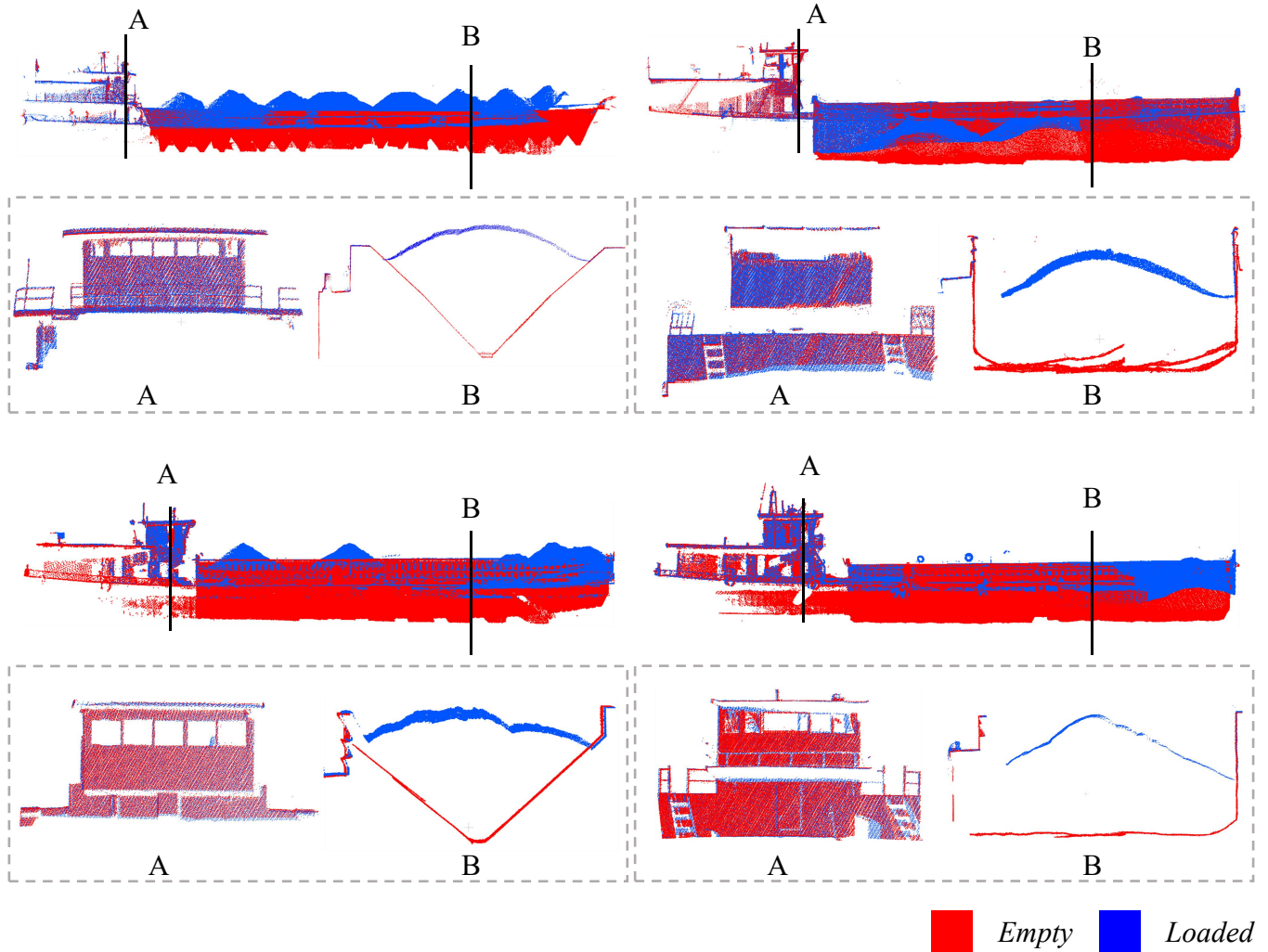


Fig. 10: Registered cargo ships with two vertical profiles for each ship shown inside the rectangles. The red and blue points indicate the empty and loaded ships, respectively.

TABLE IV: Comparison of the successful registration rate (SRR) and runtime performances between sk-4pcs [31] and the proposed method. Only the coarse registration time is recorded for sk-4pcs. The shaded rows represent the proposed method and the bold and italic cells indicate the best in the comparison.

#Ship	Methods	SRR %	Preprocessing	Runtime (s)
				Coarse registration
				Fine registration
1	sk-4pcs	0		N/A.
	proposed	100%	5.2	<i>14.6</i>
2	sk-4pcs	100%		<i>16.2</i>
	proposed	100%	6.6	22.0
3	sk-4pcs	90%		44.2
	proposed	100%	4.3	<i>9.7</i>
4	sk-4pcs	60%		74.9
	proposed	100%	6.5	<i>11.2</i>

conduct systematic evaluations with regard to the scanning speed and errors related to the floating platform.

1) *Analysis on scanning speed:* As described above, it is not possible to extend the scanning time, due to the breakage effect (Fig. 3) and limited operation time. However, shorter scanning time means fewer points and coarser spatial resolution, which inevitably degrades performance. In the

experiments above, the scanning time was empirically fixed at 36 s for the scanner [52], and to test the lower bounds of the scanning time, we generated point clouds at six different settings in the range [15,30] s with an interval of 3 s and a corresponding average mm-scale resolution.

With regard to the overall performances, our approach demonstrates strong robustness with regard to scanning speed; namely, the registration success rate does not degrade even at a scanning time of just 15 s. The translation error and rotation error range from 18 to 109 mm and 6 to 105 mdeg, respectively, as shown in Fig. 13. Although the registration accuracy decreases with faster scanning speed, this loss of accuracy is mainly caused by the coarse resolution. Specifically, for both translation and rotation errors, the registration accuracies are consistent with the resolutions of the point clouds: except for the worst case of the third cargo ship, as explained above, the translation errors are approximately the same as the average spatial resolution for the other three datasets.

2) *Analyses on the effects of moving objects:* The influences of the floating environment can be approximately categorized into (1) the noise caused by the irregular displacement between

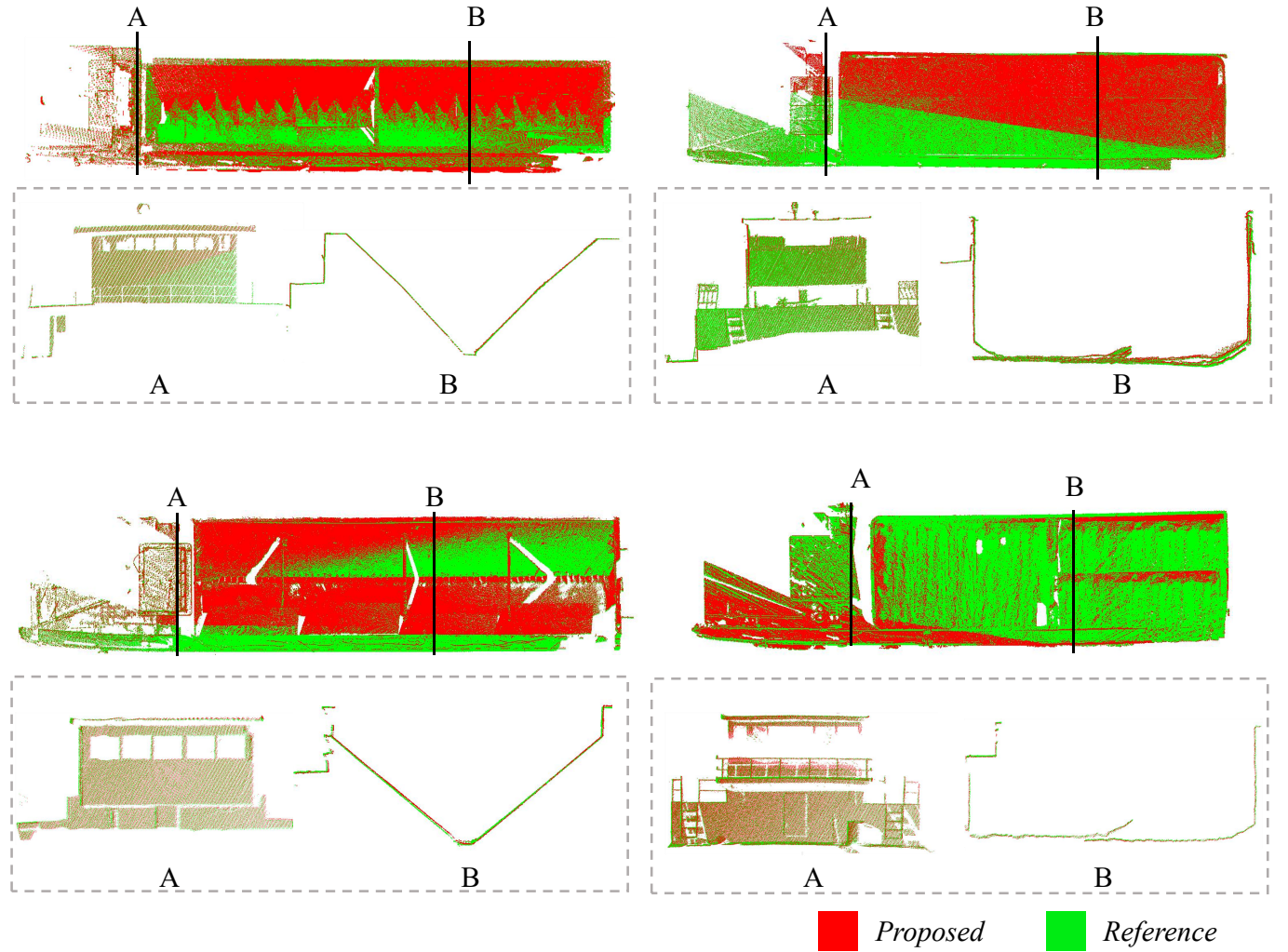


Fig. 11: Comparison between the automatic on-line pipeline and the interactive off-line registration for the ships' datasets. Two profiles are sampled for each ship.

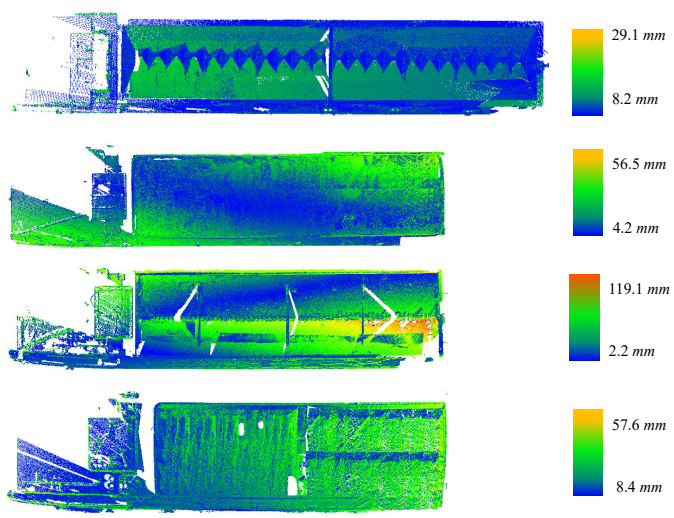


Fig. 12: Point-wise residuals after ICP registration. Note that the color scale is different for each ship, as shown in the right column.

the platform and the target cargo ship, and (2) possible periodic deformation caused by waves and other factors. In the following, we test the performances of the proposed methods against both of these factors.

a) Gaussian noises: To assess the influence of noise on the proposed approach, Gaussian noises with different standard deviations and proportions are intentionally added to the point clouds. The quantitative comparisons are displayed in Figs. 14 and 15. It can be seen that the performances for both the translation and rotation errors are almost completely uninfluenced by added Gaussian noises of all percentage magnitudes. Specifically, although there is a certain amount of fluctuation in the performances with regard to the magnitude of the noises, the fluctuations in the accuracies of the registration of point clouds are still acceptable. We deliberately select the worst results for each cargo ship and demonstrate the aligned point clouds in Fig. 16. The registered point clouds are close to each other, even in the most challenging situations.

b) Periodic perturbations: We simulate the vibration of the ships by introducing periodic height offsets for the movements of waves [54]. Specifically, the height offsets are

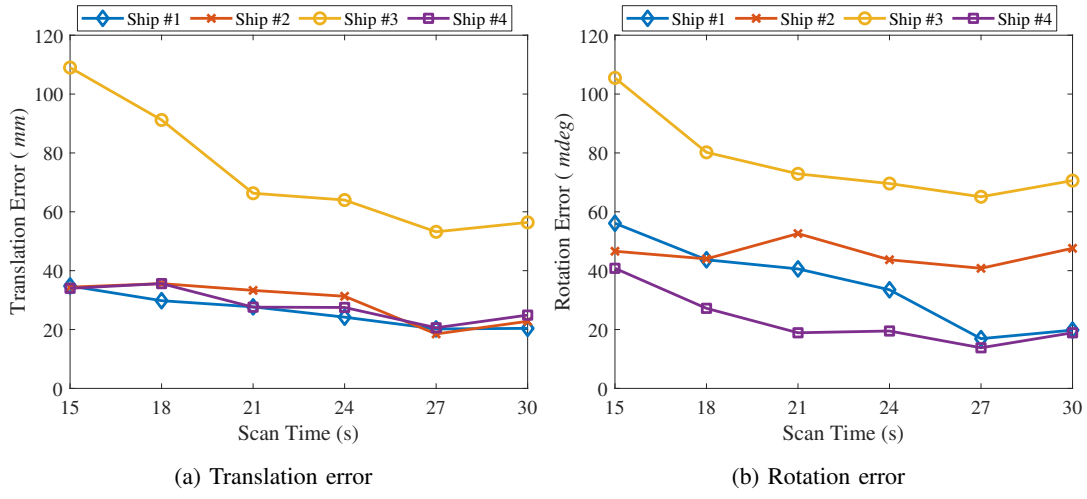


Fig. 13: Translation and rotation errors with respect to the scanning speed.

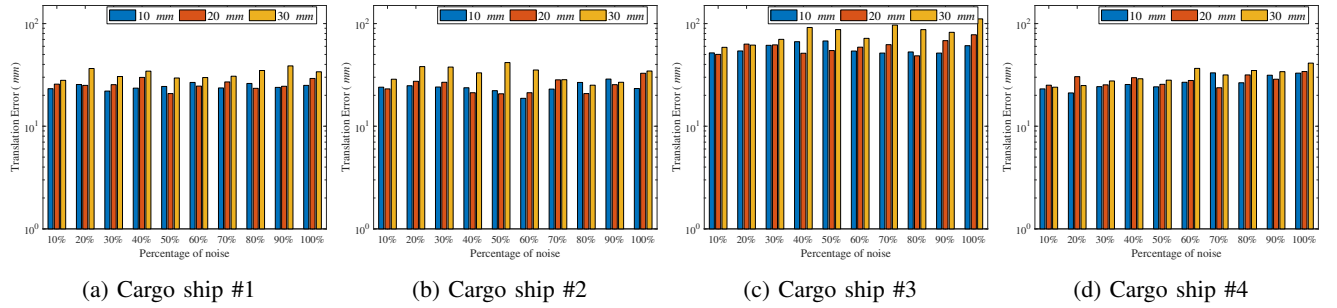


Fig. 14: Translation errors with regard to different noise levels. Different colors indicate the standard deviations of the magnitude of the Gaussian noises.

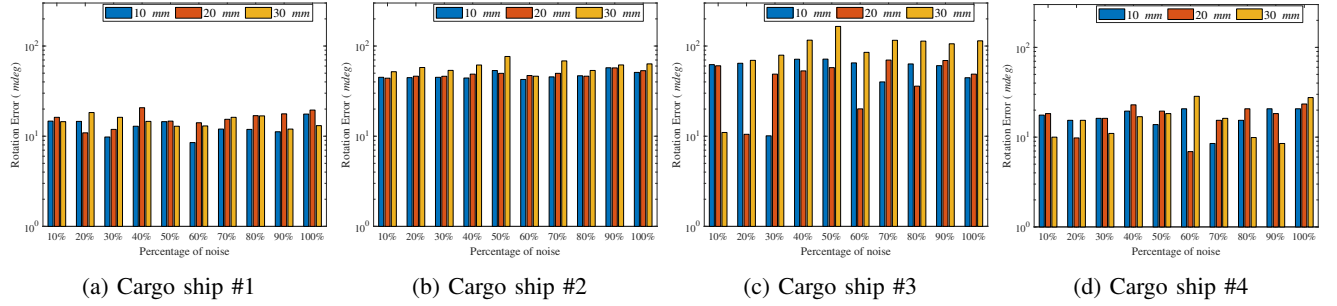


Fig. 15: Rotation errors with regard to different noise levels. Different colors indicate the standard deviations of the magnitude of the Gaussian noises.

generated by a trigonometric function within the scanning time using different frequencies and amplitudes; in addition, we use a combination of these functions to create complex functions. Fig. 17a plots a typical function and Fig. 17b shows the corresponding point clouds. Fig. 18 displays the registration results of all three states of the ships. In terms of the registration performances, the proposed method demonstrates promising robustness against the periodic perturbations.

To quantitatively evaluate the influences of a particular frequency and amplitude of vibration on the registration, we analyze the performances in terms of translation and rotation errors of the matched results for several combinations of frequency and amplitude. Figs. 19 and 20 show the translation

and rotation errors, respectively. It can be seen that the proposed approach has strong robustness against the vibrations of the ship, and achieves a high success rate for all of the tested combinations. Although the accuracies are somewhat affected, this is mainly due to the non-rigid deformation generated by the periodic offsets. Notably, lower frequencies, e.g., 0.1 Hz, generally lead to worse performances; this is logical, because vibrations with higher frequencies are similar to Gaussian noises, for which ICP is more robust to handle. The low-frequency deformations have even stronger influences when combined with larger amplitudes; this may cause the point clouds to have different observable layers after registration. However, even in this situation, we still obtain reasonable

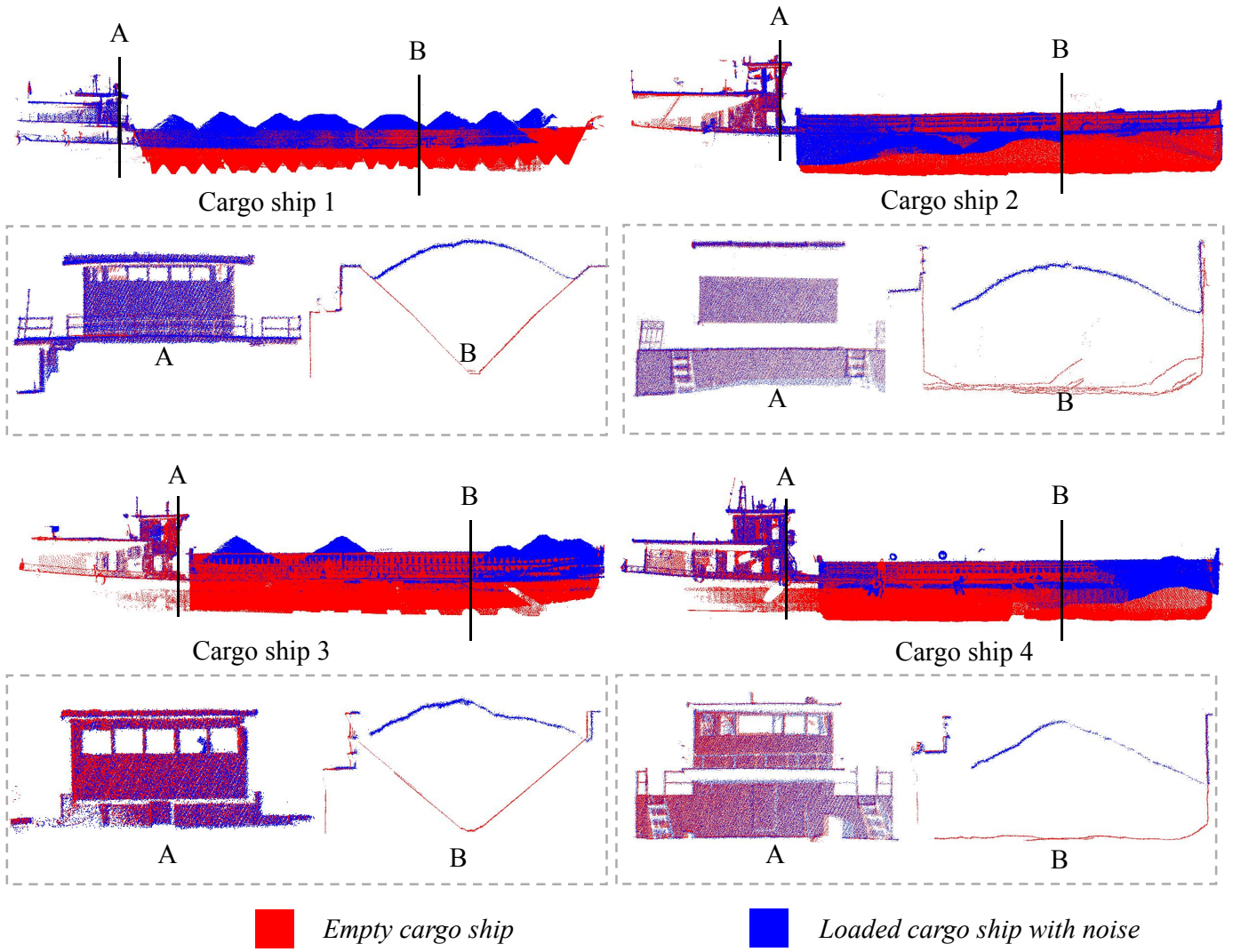


Fig. 16: Registered cargo ships with two vertical profiles for each ship shown inside the rectangles. The red and blue points indicate the point clouds for the empty ship and the noise-affected point clouds for the loaded ships, respectively.

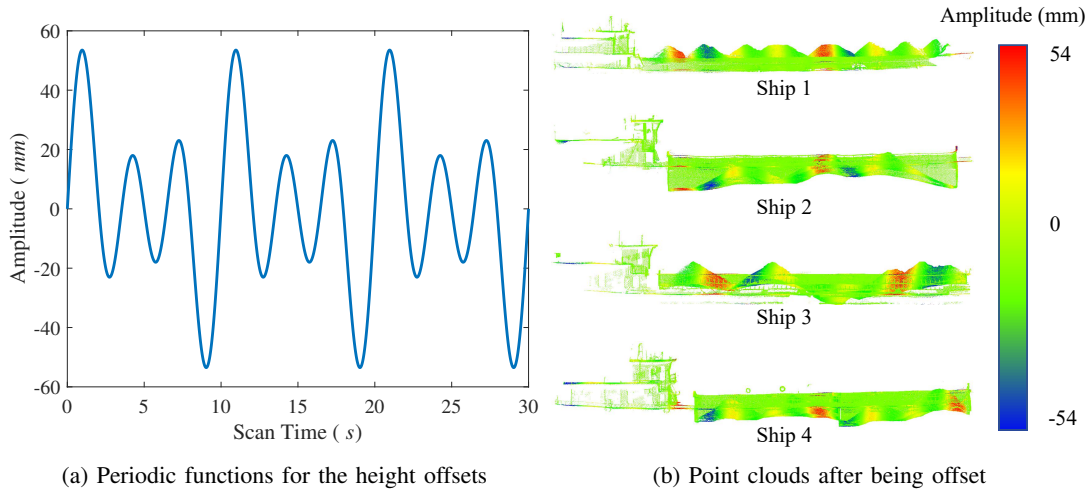


Fig. 17: The periodic functions used to generate height offset with regard to the scanning time (a) and the corresponding point clouds for the cargo ships (b). The legend indicates the amplitudes of the offsets.

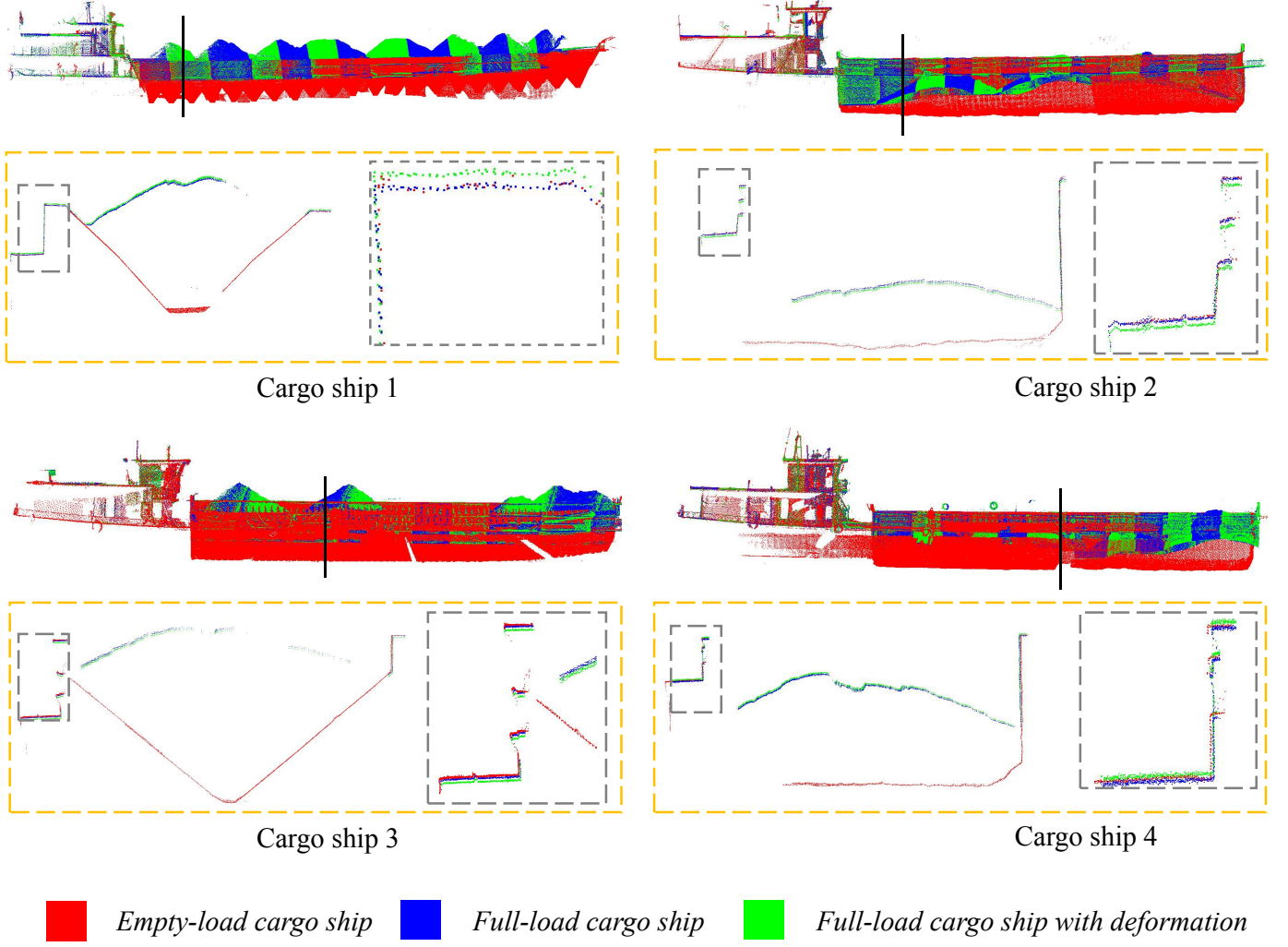


Fig. 18: Registered cargo ships for the deformed point clouds. The vertical profiles are shown inside the rectangles, and the gray rectangles are further enlargements of the profile regions.

results.

C. Discussion and Limitations

Based on the above experimental evaluations of cargo ships, we hereby discuss some properties of our method and also point out some limitations.

a) Improved robustness by structural information: Although we allow interactive selection of matching *L-Junctions* for failure cases, all of the cargo ships were automatically registered by our method in the experiments. In contrast, the 4pcs [23], k-4pcs [14] and FPFH [16] implemented in PCL [44] and Open3D [53] failed in all cases while the sk-4pcs [31] was inferior to our method in robustness. For point clouds contaminated by noise due to the unstable platform, the adoption of structural information is crucial for the robustness of the coarse registration.

b) Necessity of using static parts for ICP: Although there are a variety of methods for increasing the stability of ICP [19], [37] in cases of low overlapping ratio, pruning the changed points before ICP still improves the ICP runtime and accuracy.

c) Improved runtime efficiency using high-level features: Because silhouettes are a better abstraction of objects and contain fewer entities than semantic points [15], [31], an improvement in runtime can be expected in practical applications.

d) Limitations: Currently, only vertical planes are exploited for the extraction of silhouettes and at least two are required. In practice, it is preferable that the silhouettes cover the whole range of the objects for the proposed method; however, this requirement cannot always be fulfilled. Improved silhouettes extraction methods should be developed.

IV. CONCLUSIONS

In this paper we introduce an on-line system for the volume measurement of cargo ships, the key challenge of which is related to the registration of point clouds of these dynamic objects. This problem is elegantly solved by extracting the silhouettes of the objects and robustly registering the point clouds using the line segments and planes that comprise the silhouettes. Experimental evaluations demonstrate the superior robustness of our method and also indicate that the structural information could be used as an alternative to the semantic

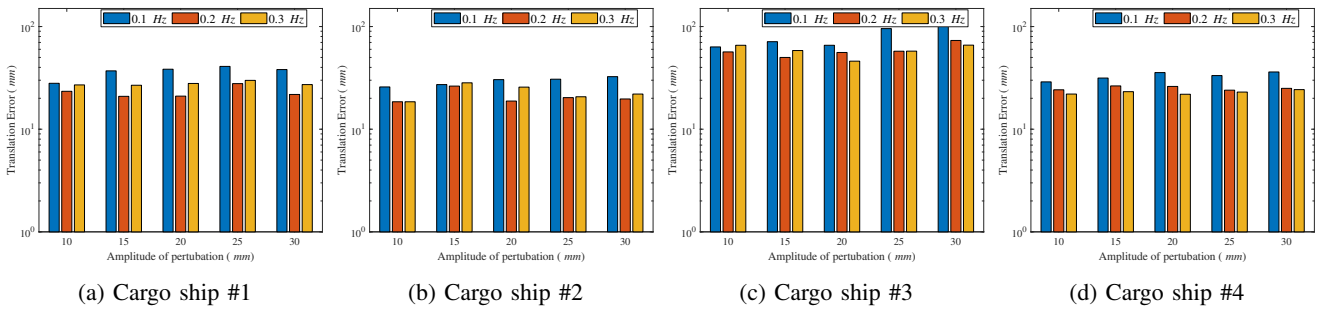


Fig. 19: Translation errors with regard to different noise levels. Different colors indicate the standard deviations of the magnitude of the Gaussian noises.

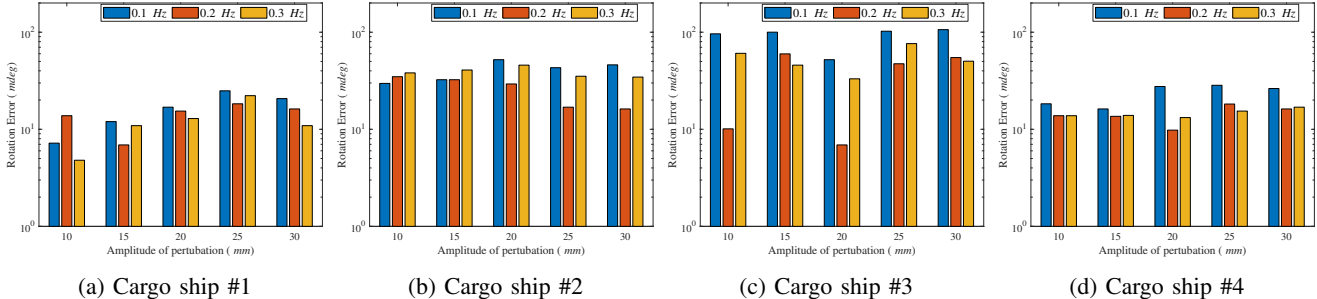


Fig. 20: Rotation errors with regard to different noise levels. Different colors indicate the standard deviations of the magnitude of the Gaussian noises.

keypoints [31], [39]. In addition, we also study the performance of our method in the context of possible problems caused by the floating platform, and find that it demonstrates strong robustness to these factors. However, the current methods of silhouette extraction impose constraints on the scenes, e.g., vertical planes are required. Thus, more robust approaches should be explored in the future by using learning methods to systematically understanding the scenes [55]. Furthermore, it will be interesting to exploit the proposed strategy for the registration of point clouds in urban environments [56], in which the silhouettes of buildings could be used to increase both the efficiency and reliability of the registration.

REFERENCES

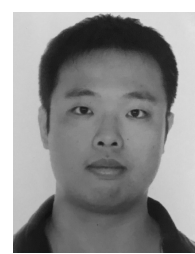
- [1] L. Nan, A. Sharf, H. Zhang, D. Cohen-Or, and B. Chen, "Smartboxes for interactive urban reconstruction," in *ACM Transactions on Graphics (TOG)*, vol. 29, no. 4. ACM, 2010, p. 93.
- [2] P. Musialski, P. Wonka, D. G. Aliaga, M. Wimmer, L. Van Gool, and W. Purgathofer, "A survey of urban reconstruction," in *Computer graphics forum*, vol. 32, no. 6. Wiley Online Library, 2013, pp. 146–177.
- [3] X. Liang, V. Kankare, J. Hyppä, Y. Wang, A. Kukko, H. Haggrén, X. Yu, H. Kaartinen, A. Jaakkola, F. Guan *et al.*, "Terrestrial laser scanning in forest inventories," *ISPRS Journal of Photogrammetry and Remote Sensing*, vol. 115, pp. 63–77, 2016.
- [4] N. Saarinen, V. Kankare, M. Vastaranta, V. Luoma, J. Pyörälä, T. Tamhuanpää, X. Liang, H. Kaartinen, A. Kukko, A. Jaakkola *et al.*, "Feasibility of terrestrial laser scanning for collecting stem volume information from single trees," *ISPRS journal of photogrammetry and remote sensing*, vol. 123, pp. 140–158, 2017.
- [5] M. Vaaja, M. Kurkela, J.-P. Virtanen, M. Maksimainen, H. Hyppä, J. Hyppä, and E. Tetri, "Luminance-corrected 3d point clouds for road and street environments," *Remote Sensing*, vol. 7, no. 9, pp. 11 389–11 402, 2015.
- [6] B. Yang, Z. Dong, Y. Liu, F. Liang, and Y. Wang, "Computing multiple aggregation levels and contextual features for road facilities recognition using mobile laser scanning data," *ISPRS Journal of Photogrammetry and Remote Sensing*, vol. 126, pp. 180–194, 2017.
- [7] R. Qin and A. Gruen, "3d change detection at street level using mobile laser scanning point clouds and terrestrial images," *ISPRS Journal of Photogrammetry and Remote Sensing*, vol. 90, pp. 23–35, 2014.
- [8] X. Ge, "Terrestrial laser scanning technology from calibration to registration with respect to deformation monitoring," Ph.D. dissertation, Technische Universität München, 2016.
- [9] L. Cheng, S. Chen, X. Liu, H. Xu, Y. Wu, M. Li, and Y. Chen, "Registration of laser scanning point clouds: A review," *Sensors*, vol. 18, no. 5, p. 1641, 2018.
- [10] Z. Dong, B. Yang, F. Liang, R. Huang, and S. Scherer, "Hierarchical registration of unordered tls point clouds based on binary shape context descriptor," *ISPRS journal of photogrammetry and remote sensing*, vol. 144, pp. 61–79, 2018.
- [11] Z. Cai, T.-J. Chin, A. P. Bustos, and K. Schindler, "Practical optimal registration of terrestrial lidar scan pairs," *ISPRS journal of photogrammetry and remote sensing*, vol. 147, pp. 118–131, 2019.
- [12] X. Ge, H. Hu, and B. Wu, "Image-guided registration of unordered terrestrial laser scanning point clouds for urban scenes," *IEEE Transactions on Geoscience and Remote Sensing*, vol. (in press), 2019.
- [13] N. Mellado, D. Aiger, and N. J. Mitra, "Super 4pcs fast global pointcloud registration via smart indexing," in *Computer Graphics Forum*, vol. 33, no. 5. Wiley Online Library, 2014, pp. 205–215.
- [14] P. W. Theiler, J. D. Wegner, and K. Schindler, "Keypoint-based 4-points congruent sets-automated marker-less registration of laser scans," *ISPRS journal of photogrammetry and remote sensing*, vol. 96, pp. 149–163, 2014.
- [15] B. Yang, Z. Dong, F. Liang, and Y. Liu, "Automatic registration of large-scale urban scene point clouds based on semantic feature points," *ISPRS Journal of Photogrammetry and Remote Sensing*, vol. 113, pp. 43–58, 2016.
- [16] Q.-Y. Zhou, J. Park, and V. Koltun, "Fast global registration," in *European Conference on Computer Vision*. Springer, 2016, pp. 766–782.
- [17] Z. Dong, B. Yang, Y. Liu, F. Liang, B. Li, and Y. Zang, "A novel binary shape context for 3d local surface description," *ISPRS Journal of Photogrammetry and Remote Sensing*, vol. 130, pp. 431–452, 2017.

- [18] P. J. Besl and N. D. McKay, "Method for registration of 3-d shapes," in *Sensor fusion IV: control paradigms and data structures*, vol. 1611. International Society for Optics and Photonics, 1992, pp. 586–606.
- [19] K.-L. Low, "Linear least-squares optimization for point-to-plane icp surface registration," *Chapel Hill, University of North Carolina*, vol. 4, no. 10, pp. 1–3, 2004.
- [20] J. Yang, H. Li, and Y. Jia, "Go-icp: Solving 3d registration efficiently and globally optimally," in *Proceedings of the IEEE International Conference on Computer Vision*, 2013, pp. 1457–1464.
- [21] Autodesk, "Recap," <https://www.autodesk.com/products/recap/overview>, 2019, accessed: Jul 13th.
- [22] FARO, "Faro scene," <https://www.faro.com/products/construction-bim-cim/faro-scene/>, 2019, accessed: Jul 13.
- [23] D. Aiger, N. J. Mitra, and D. Cohen-Or, "4-points congruent sets for robust pairwise surface registration," in *ACM transactions on graphics (TOG)*, vol. 27, no. 3. ACM, 2008, p. 85.
- [24] S. Barnea and S. Filin, "Keypoint based autonomous registration of terrestrial laser point-clouds," *ISPRS Journal of Photogrammetry and Remote Sensing*, vol. 63, no. 1, pp. 19–35, 2008.
- [25] M. A. Fischler and R. C. Bolles, "Random sample consensus: a paradigm for model fitting with applications to image analysis and automated cartography," *Communications of the ACM*, vol. 24, no. 6, pp. 381–395, 1981.
- [26] R. B. Rusu, N. Blodow, and M. Beetz, "Fast point feature histograms (fpfh) for 3d registration," in *2009 IEEE International Conference on Robotics and Automation*. IEEE, 2009, pp. 3212–3217.
- [27] T. Weber, R. Hänsch, and O. Hellwich, "Automatic registration of unordered point clouds acquired by kinect sensors using an overlap heuristic," *ISPRS Journal of Photogrammetry and Remote Sensing*, vol. 102, pp. 96–109, 2015.
- [28] I. Sipiran and B. Bustos, "Harris 3d: a robust extension of the harris operator for interest point detection on 3d meshes," *The Visual Computer*, vol. 27, no. 11, p. 963, 2011.
- [29] J. Knopp, M. Prasad, G. Willems, R. Timofte, and L. Van Gool, "Hough transform and 3d surf for robust three dimensional classification," in *European Conference on Computer Vision*. Springer, 2010, pp. 589–602.
- [30] D. G. Lowe, "Distinctive image features from scale-invariant keypoints," *International journal of computer vision*, vol. 60, no. 2, pp. 91–110, 2004.
- [31] X. Ge, "Automatic markerless registration of point clouds with semantic-keypoint-based 4-points congruent sets," *ISPRS Journal of Photogrammetry and Remote Sensing*, vol. 130, pp. 344–357, 2017.
- [32] A. Segal, D. Haehnel, and S. Thrun, "Generalized-icp," in *Robotics: science and systems*, vol. 2, no. 4. Seattle, WA, 2009, p. 435.
- [33] G. Xu, S. Du, D. Cui, S. Zhang, B. Chen, X. Zhang, J. Xue, and Y. Gao, "Precise point set registration using point-to-plane distance and correntropy for lidar based localization," in *2018 IEEE Intelligent Vehicles Symposium (IV)*. IEEE, 2018, pp. 734–739.
- [34] M. Magnusson, A. Lilienthal, and T. Duckett, "Scan registration for autonomous mining vehicles using 3d-ndt," *Journal of Field Robotics*, vol. 24, no. 10, pp. 803–827, 2007.
- [35] A. Das, J. Servos, and S. L. Waslander, "3d scan registration using the normal distributions transform with ground segmentation and point cloud clustering," in *2013 IEEE International Conference on Robotics and Automation*. IEEE, 2013, pp. 2207–2212.
- [36] J. Park, Q.-Y. Zhou, and V. Koltun, "Colored point cloud registration revisited," in *Proceedings of the IEEE International Conference on Computer Vision*, 2017, pp. 143–152.
- [37] D. Chetverikov, D. Svirko, D. Stepanov, and P. Krsek, "The trimmed iterative closest point algorithm," in *Object recognition supported by user interaction for service robots*, vol. 3. IEEE, 2002, pp. 545–548.
- [38] Z. Xu, E. Xu, Z. Zhang, and L. Wu, "Multiscale sparse features embedded 4-points congruent sets for global registration of tis point clouds," *IEEE Geoscience and Remote Sensing Letters*, vol. 16, no. 2, pp. 286–290, 2018.
- [39] B. Yang, Y. Zang, Z. Dong, and R. Huang, "An automated method to register airborne and terrestrial laser scanning point clouds," *ISPRS journal of photogrammetry and remote sensing*, vol. 109, pp. 62–76, 2015.
- [40] B. Fan, F. Wu, and Z. Hu, "Robust line matching through line-point invariants," *Pattern Recognition*, vol. 45, no. 2, pp. 794–805, 2012.
- [41] M. Hofer, M. Maurer, and H. Bischof, "Efficient 3d scene abstraction using line segments," *Computer Vision and Image Understanding*, vol. 157, pp. 167–178, 2017.
- [42] K. Li, J. Yao, X. Lu, L. Li, and Z. Zhang, "Hierarchical line matching based on line-junction-line structure descriptor and local homography estimation," *Neurocomputing*, vol. 184, pp. 207–220, 2016.
- [43] B. Wu, Y. Zhang, and Q. Zhu, "Integrated point and edge matching on poor textual images constrained by self-adaptive triangulations," *ISPRS journal of photogrammetry and remote sensing*, vol. 68, pp. 40–55, 2012.
- [44] R. B. Rusu and S. Cousins, "Point cloud library (pcl)," in *2011 IEEE international conference on robotics and automation*, 2011, pp. 1–4.
- [45] Q. Zhu, F. Wang, H. Hu, Y. Ding, J. Xie, W. Wang, and R. Zhong, "Intact planar abstraction of buildings via global normal refinement from noisy oblique photogrammetric point clouds," *ISPRS International Journal of Geo-Information*, vol. 7, no. 11, p. 431, 2018.
- [46] R. Schnabel, R. Wahl, and R. Klein, "Efficient ransac for point-cloud shape detection," in *Computer graphics forum*, vol. 26, no. 2. Wiley Online Library, 2007, pp. 214–226.
- [47] F. Bernardini and C. L. Bajaj, "Sampling and reconstructing manifolds using alpha-shapes," 1997.
- [48] L. Xie, Q. Zhu, H. Hu, B. Wu, Y. Li, Y. Zhang, and R. Zhong, "Hierarchical regularization of building boundaries in noisy aerial laser scanning and photogrammetric point clouds," *Remote Sensing*, vol. 10, no. 12, p. 1996, 2018.
- [49] L. Wang, U. Neumann, and S. You, "Wide-baseline image matching using line signatures," in *2009 IEEE 12th International Conference on Computer Vision*. IEEE, 2009, pp. 1311–1318.
- [50] L. Zhang and R. Koch, "An efficient and robust line segment matching approach based on lbd descriptor and pairwise geometric consistency," *Journal of Visual Communication and Image Representation*, vol. 24, no. 7, pp. 794–805, 2013.
- [51] L. Moisan, P. Moulon, and P. Monasse, "Automatic homographic registration of a pair of images, with a contrario elimination of outliers," *Image Processing On Line*, vol. 2, pp. 56–73, 2012.
- [52] HiCloud. (2019) Hs450 precision laser scanner. <http://www.hicloud.com.cn/html/hardware/2015-10-15/1054.html>. Accessed: August 13th.
- [53] Q.-Y. Zhou, J. Park, and V. Koltun, "Open3d: A modern library for 3d data processing," *arXiv preprint arXiv:1801.09847*, 2018.
- [54] T. R. Lin, J. Pan, P. J. O'Shea, and C. K. Mechefske, "A study of vibration and vibration control of ship structures," *Marine Structures*, vol. 22, no. 4, pp. 730–743, 2009.
- [55] C. R. Qi, L. Yi, H. Su, and L. J. Guibas, "Pointnet++: Deep hierarchical feature learning on point sets in a metric space," in *Advances in neural information processing systems*, 2017, pp. 5099–5108.
- [56] W. Tao, X. Hua, Z. Chen, and P. Tian, "Fast and automatic registration of terrestrial point clouds using 2d line features," *Remote Sensing*, vol. 12, no. 8, p. 1283, 2020.

Feng Wang received a B.S. degree in the School of Remote Sensing and Information Engineering, Wuhan University in 2014. He is currently a Ph.D. candidate in the Faculty of Geosciences and Environmental Engineering, Southwest Jiaotong University. His research interests include photogrammetry, point clouds processing and 3D modeling.



Han Hu received B.S. and Ph.D. degrees at the School of Remote Sensing and Information Engineering and State Key Laboratory of Information Engineering in Surveying, Mapping and Remote Sensing, Wuhan University, in 2010 and 2015, respectively. He served as a Postdoctoral Fellow at the Hong Kong Polytechnic University from 2015 to 2019.



He is currently a Professor in the Faculty of Geosciences and Environmental Engineering, Southwest Jiaotong University. His research interests include photogrammetry, point clouds processing and 3D modeling.



Xuming Ge received a Ph.D. degree in the Geodesy from the Technical University of Munich, Germany, in 2016.

He is now an Associate Professor in the Faculty of Geosciences and Environmental Engineering of Southwest Jiaotong University, mainly working on point clouds registration and classification. His research interests include photogrammetry, 3D reconstruction, point clouds processing and sensor calibration.



Qing Zhu received B.S. and M.S. degrees in Aerial Photogrammetry in 1986 and 1989, respectively, from Southwest University, and a Ph.D. degree in Railway Engineering in 1995 from North Jiaotong University. Since 1997, he had worked as a Professor at the State Key Laboratory of Information Engineering in Surveying, Mapping and Remote Sensing, Wuhan University and received the Cheung Kong Scholars in 2009.

Since 2014 he has been a Professor and the Director of the Research Committee at the Faculty of Geosciences and Environmental Engineering, Southwest Jiaotong University. He also serves as a Visiting Professor for Wuhan University, Central South University and Chongqing University. He is the Editor-in-Chief of the *Journal of Smart Cities* and also serves on the Editorial Board of more than 10 journals, including *Computers, Environment and Urban Systems*, *Transactions in GIS* and *International Journal of 3D Information*. He has authored or co-authored more than 260 articles and seven books. His research interests include photogrammetry, GIS and virtual geographic environments.



Bo Xu received a Ph.D. degree in the Information Engineering and State Key Laboratory of Information Engineering in Surveying, Mapping and Remote Sensing, Wuhan University, in 2016.

He is now a Research Associate in the Faculty of Geosciences and Environmental Engineering of Southwest Jiaotong University. Before that, he worked as a Postdoctoral Fellow for Purdue University. His research interests are in 3D point cloud processing and building reconstruction.



Ruofei Zhong received a Ph.D. degree in Geo-Informatics from Institute of Remote Sensing Applications, Chinese Academy of Sciences in 2005.

He is currently a Professor with the Beijing Advanced Innovation Center for Imaging Technology and Key Laboratory of 3D Information Acquisition and Application, College of Resource Environment and Tourism, Capital Normal University. His research interests include LiDAR processing and system development for laser scanners.



Yulin Ding received B.S. and Ph.D. degrees in the School of Resource and Environmental Sciences and State Key Laboratory of Information Engineering in Surveying, Mapping and Remote Sensing, Wuhan University, in 2009 and 2014, respectively.

She is currently an Associate Professor in the Faculty of Geosciences and Environmental Engineering, Southwest Jiaotong University. Her research interests mainly include virtual geographic environments, 3D GIS, and big data.



Xiao Xie received a Ph.D. degree from Wuhan University in 2016, and now serves as a Senior Engineer at Zhejiang Hi-target Space Information Technology Co., Ltd. She is also an Assistant Professor in Urban and Environmental Computation at the Institute of Applied Ecology, Chinese Academy of Sciences. Her research interests include 3D GIS and smart cities.